SUPPLEMENTARY INFORMATION

"Quaternary climate modulation of Pb isotopes in the deep Indian Ocean linked to the Himalayan chemical weathering" by Wilson D.J., Galy A., Piotrowski A.M., and Banakar V.K.

1. Age model

The age model for SK129-CR2 is constrained by planktonic radiocarbon dates for 0-33 ka BP (Table S1), beyond which the benthic foraminiferal *C. wuellerstorfi* $\delta^{18}O$ record (Table S2) is tuned to the LR04 benthic $\delta^{18}O$ stack (Lisiecki and Raymo, 2005) at major marine isotope stage (MIS) boundaries. Linear interpolation was used between all radiocarbon and benthic $\delta^{18}O$ tie points. The depth-age tie points and linear sedimentation rates are detailed in Table S3. We note that the LR04 record has an absolute age uncertainty of ~4 kyr over this time period (Lisiecki and Raymo, 2005).

2. Chemical purification and mass spectrometry – complete method details

The Pb fraction was separated using BioRad AG1-X8 anion exchange resin (100-200 μm mesh) in 100 μl Teflon columns in laminar flow hoods using quartz-distilled acids. The columns were washed with 6M HCl and primed with 0.7M HBr before samples were loaded in 0.7M HBr. After washing with 0.7M HBr and 2M HCl, the Pb was eluted in 6M HCl and dried down, before being taken up in 2% HNO_3 for analysis by mass spectrometry.

The Pb isotopic composition was analysed on a Nu Plasma multi-collector inductively-coupled plasma mass spectrometer (MC-ICP-MS) in the Department of Earth Sciences at the University of Cambridge. Thallium (Tl) was used as an internal standard to correct for mass fractionation (Hirata, 1996; Belshaw et al., 1998) according to an exponential law. The reliability of this approach was optimised by using matrix- and concentration-matched standards and samples (Rehkamper and Mezger, 2000), spiking with a constant Pb/Tl ratio (~2) and mixing Pb and Tl immediately prior to analysis (Kamenov et al., 2004). The mercury (Hg) beam was also monitored at mass 202, allowing for an interference correction for the ^{204}Hg on ^{204}Pb using the natural $^{204}Hg/^{202}Hg$ ratio, itself corrected for mass fractionation assessed by Tl and using an exponential law.

Concentration-matched NIST-SRM-981 Pb standards were measured after approximately every five samples, and a linear correction was applied to all data measured in each analytical session in order to produce agreement with the accepted composition of NIST-SRM-981 Pb (Galer and Abouchami, 1998; Abouchami et al., 2000). The standard deviation (2σ) of repeat measurements of NIST-SRM-981 measured and Tl-corrected as a sample provides our external reproducibility for samples analysed during each analytical session, giving reproducibility in the range of 30-180 ppm for $^{206}Pb/^{204}Pb$, 60-240 ppm for $^{207}Pb/^{204}Pb$ and 50-250 ppm for $^{208}Pb/^{204}Pb$. Two internal standards (leachate samples that had been through column chemistry) were also analysed in multiple analytical sessions over three years (n=14-15) and yield typical long term reproducibility (2σ) of 140 ppm for $^{206}Pb/^{204}Pb$, 160 ppm for $^{207}Pb/^{204}Pb$ and 190 ppm for $^{208}Pb/^{204}Pb$. For 11 samples, replicates were analysed in two separate analytical sessions and give results that are consistent with that external reproducibility (Table S4).

Full procedural blanks for the sediment leaching were 1.9 ± 0.7 ng (1σ, n=9). Blanks analysed for isotopic composition gave average values of $^{206}Pb/^{204}Pb$ = 18.11 ± 0.44, $^{207}Pb/^{204}Pb$ = 15.56 ± 0.07 and $^{208}Pb/^{204}Pb$ = 37.77 ± 0.33 (1σ, n=7), consistent with a mixture between sample Pb and anthropogenic Pb with an approximately Broken Hill composition (Stacey et al., 1969). Leachate samples typically contained 400-1000 ng Pb, so the blank contribution represents only 0.2-0.5% of the total Pb. Therefore, no blank correction has been applied. In the smallest samples analysed, which contained ~200 ng Pb, the blank could contribute up to ~1% of the Pb and produce an error of ~100 ppm for $^{207}Pb/^{204}Pb$ and ~ 400 ppm for $^{206}Pb/^{204}Pb$ and $^{208}Pb/^{204}Pb$. This error is comparable to the external analytical reproducibility, and remains negligible in comparison to downcore variability in SK129-CR2, which is ~30 times larger.

3. Assessing anthropogenic contamination of sediment leachates

All measured leachate Pb isotope data from SK129-CR2 (Table S4) are plotted against core depth in Figure S1 and as Pb-Pb plots in Figure S2. These data reveal changes through time across two full glacial cycles that mostly fall on a binary mixing line in Pb-Pb space. Within the depth range from 60-518 cm, most samples form a relatively smooth pattern of temporal variability, but six samples out of 82 fall significantly outside of that smooth pattern, in each case towards less radiogenic Pb isotopic compositions (Figure S1). These samples also lie significantly away from the binary mixing line defined by the other samples in $^{207}Pb/^{204}Pb$ v $^{206}Pb/^{204}Pb$ space (Figure S2), with higher $^{207}Pb/^{204}Pb$ for a given $^{206}Pb/^{204}Pb$. In contrast, any such divergence away from binary mixing is less apparent in $^{208}Pb/^{204}Pb$ v $^{206}Pb/^{204}Pb$ space. Together, these observations appear to indicate anthropogenic contamination by a contaminant with approximately the Broken Hill composition (Stacey et al., 1969) (Figure S2), which has been shown to be the main source of anthropogenic Pb for the 20th century (van de Velde et al., 2005).

Whereas such contamination from 60-518 cm appears to be occasional and distributed randomly, in the upper section of the core (8-56 cm) the majority of samples appear to deviate away from the binary mixing line, also in a similar direction (Figure S2). This behaviour produces a somewhat spiky time series (Figure S1) and a smaller magnitude of deglacial change for Termination I than for the other glacial-interglacial transitions in the record, especially for $^{208}Pb/^{204}Pb$ and $^{206}Pb/^{204}Pb$. These observations are also consistent with anthropogenic contamination. However, the amount of contamination that would be required is considerably larger than can be explained by any of our measured procedural blanks (Section 3.3 of the main text) and there is not such a persistent artifact in the remainder of the leachate record. We therefore suggest that the contamination in the 8-56 cm section of the core likely occurred during coring or core storage and processing, rather than during leaching in the laboratory.

For those samples described above for which we suspect anthropogenic contamination, we have attempted to make a correction by regressing from the Broken Hill composition (Stacey et al., 1969), which is taken to represent the most likely composition for the anthropogenic contaminant, onto the best-fit binary mixing line through the data from the remaining 76 samples (Figure S2). As can be seen in Figure S1, the correction is relatively larger for $^{208}Pb/^{204}Pb$ and $^{206}Pb/^{204}Pb$ than for $^{207}Pb/^{204}Pb$. The corrected data for the 8-56 cm section show a smoother pattern of change across Termination I (Figure S1) and a similar magnitude of glacial-interglacial variability to that observed at previous terminations. For the other six samples suspected to be contaminated, this correction also leads to a significant improvement, since on average the divergence from the temporal patterns of $^{208}Pb/^{204}Pb$ and $^{206}Pb/^{204}Pb$ defined by the remainder of the data is reduced by ~80 % (Figure S1). The apparent improvement of the corrected data over the raw data in terms of autocorrelation between adjacent samples further supports our suggestion of anthropogenic contamination.

Since we are uncertain of the source or isotopic composition of the contaminant, those six outlying data points (Figure S1) are excluded from further discussion. For the 8-56 cm section of the record, our correction appears reasonably robust and we include the corrected data in Table S5. Those corrected data from 8-56 cm are plotted in the time series plots, but are not plotted in the Pb-Pb plots because the mixing trend is well defined by the 76 measured data not requiring a correction.

4. Sediment leaching reproducibility

We tested the effect of sample size during leaching (Wilson et al., 2013) in the case of one glacial sample (328 cm) and one interglacial sample (434 cm) from SK129-CR2 (Table S4). At 328 cm, the smaller sample is less radiogenic by ~ 1000 ppm, 350 ppm and 550 ppm for $^{206}Pb/^{204}Pb$, $^{207}Pb/^{204}Pb$ and $^{208}Pb/^{204}Pb$ respectively (Figure S1), which is larger than the measurement uncertainty. The direction of change is consistent with a minor volcanic contamination of the smaller sample, as suggested previously for Nd isotopes (Wilson et al., 2013), but the magnitude is only ~10 % of the magnitude of glacial-interglacial Pb isotope changes. At 434 cm, the smaller sample is instead more radiogenic than the larger sample (Figure S1), which is not the direction expected for volcanic contamination. Since we suggested that the large sample at 434 cm may have been affected by anthropogenic contamination, it is hard to assess the reproducibility related to sample size in this case. Overall, this sample size test should represent a worst case scenario, and suggests that less than 10 % of the glacial-interglacial variability in the record may be explained by leaching systematics.

In a second test, we used low solution/solid ratios to prevent complete decarbonation before HH leaching on a subset of 9 samples (Table S4). There is excellent agreement for Pb isotopes between these data and the remainder of the data measured on decarbonated leachates. Given evidence that the use of low solution/solid ratios is a more reliable approach for deep sea authigenic Nd isotope reconstructions (Wilson et al., 2013), this good agreement provides further confidence in our Pb isotope reconstruction.

Overall, the above tests suggest a generally reliable recovery of the authigenic Pb isotope signal by sediment leaching in core SK129-CR2, in agreement with a more general mass balance argument that leaching should be more robust for Pb isotopes than for Nd isotopes (Gutjahr et al., 2007).

5. Detrital sediment Pb isotopic composition of the Lower Meghna

Sample BGP 21 was collected from the Lower Meghna during the monsoon period and represents the whole silicate fraction of the suspended load. It was leached with 1 M acetic acid to remove authigenic components before dissolution and measurement of its Pb isotopic composition (Galy and France-Lanord, 2001). Its Pb isotopic composition is $^{206}Pb/^{204}Pb = 19.297 \pm 0.005$, $^{207}Pb/^{204}Pb = 15.796 \pm 0.005$, $^{208}Pb/^{204}Pb = 39.72 \pm 0.01$ (all 2σ errors).

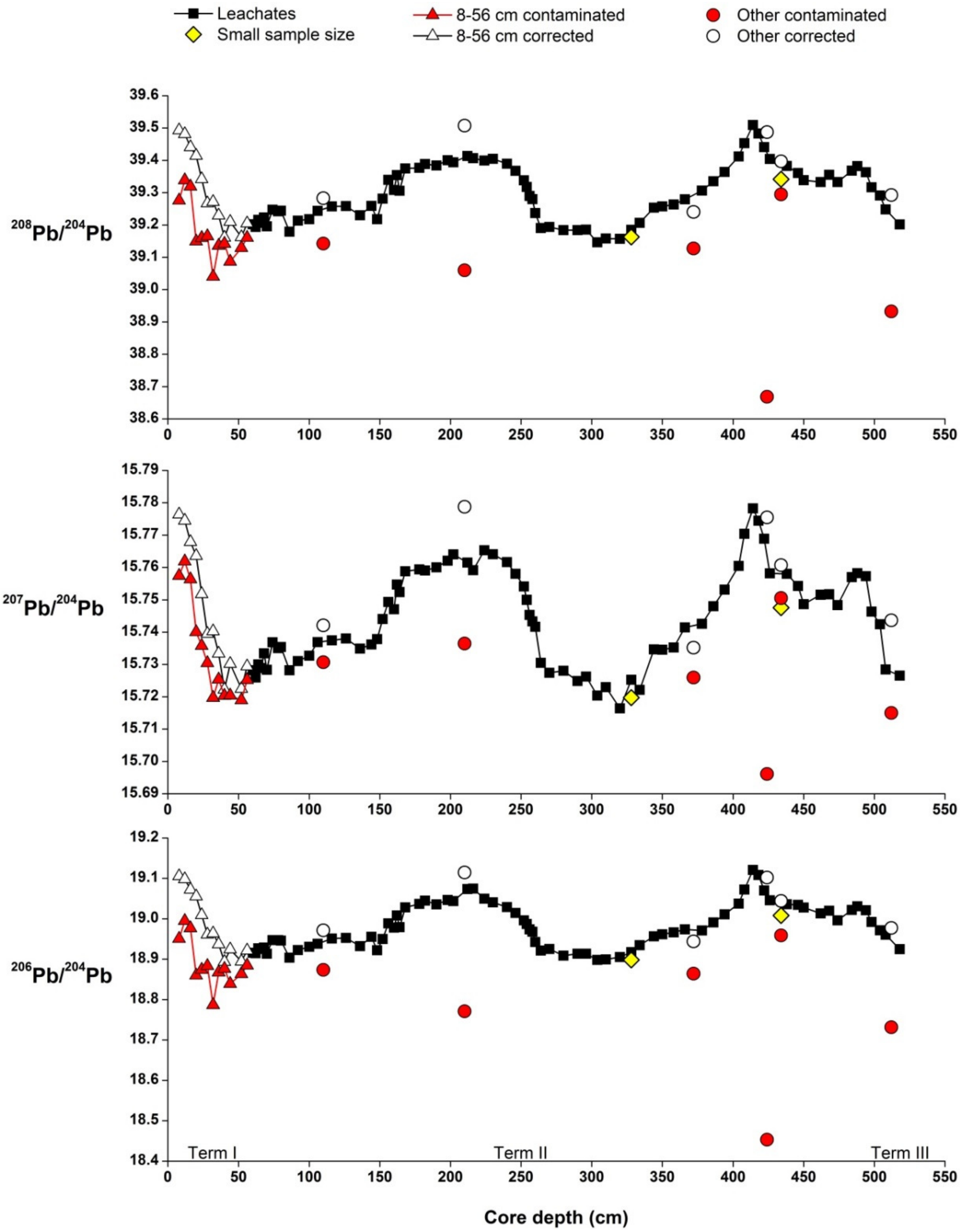

Figure S1: Sediment leachate Pb isotope data from SK129-CR2 plotted against core depth. Panels show $^{208}Pb/^{204}Pb$, $^{207}Pb/^{204}Pb$ and $^{206}Pb/^{204}Pb$ records. The leachate data considered reliable are plotted as black squares and a line. Small sample size tests at 328 cm and 434 cm are plotted as yellow diamonds. Anthropogenic contamination is suspected for the top section of the core (8-56 cm) and six other samples: the raw data are shown as red triangles and circles, and the data corrected for anthropogenic contamination (assuming a Broken Hill composition; see Figure S2) are shown as white triangles and circles. The approximate position of Terminations I, II and III within the core are shown along the x axis.

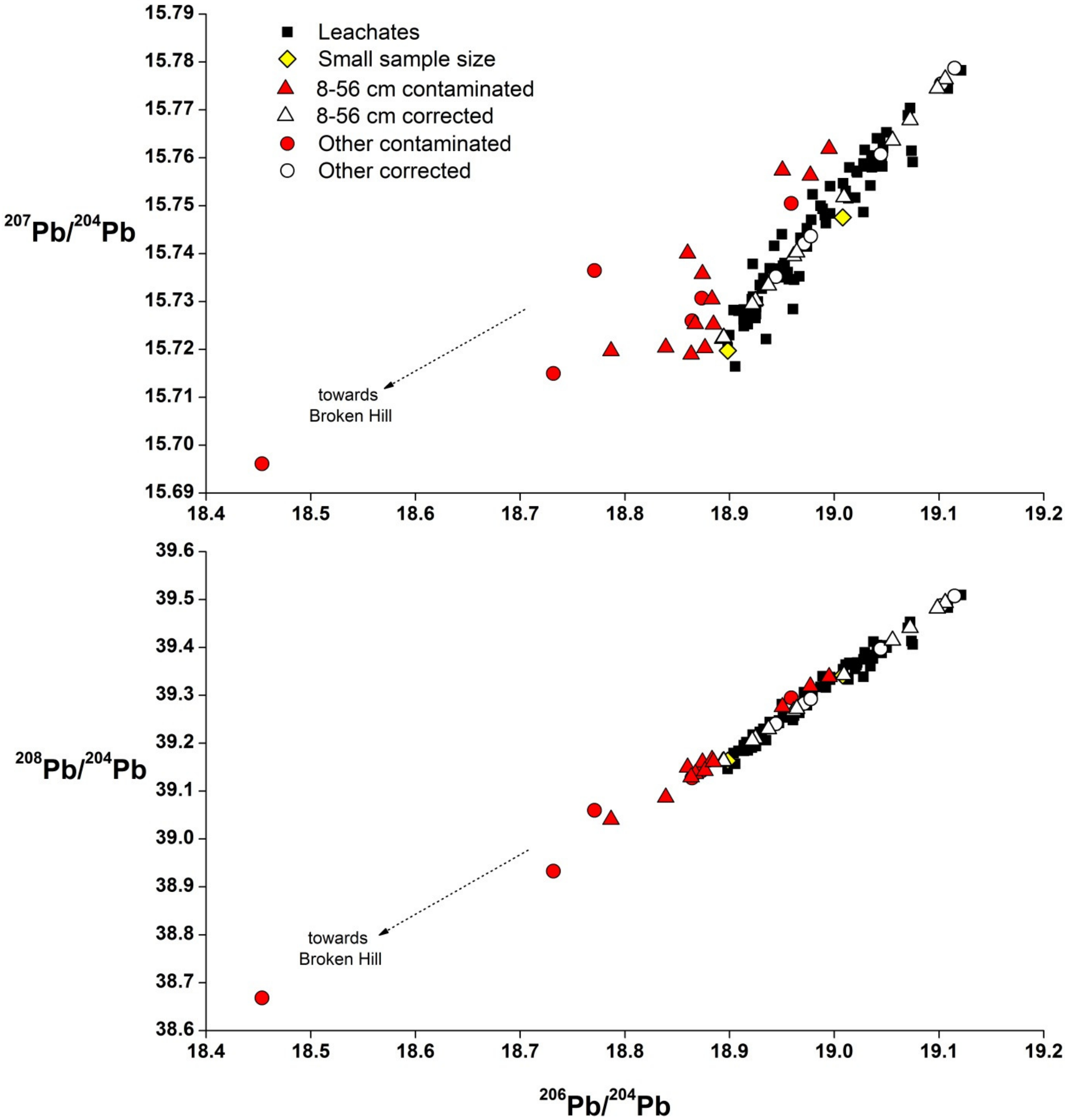

Figure S2: Sediment leachate Pb isotope data from SK129-CR2 plotted as Pb-Pb crossplots: $^{207}Pb/^{204}Pb$ versus $^{206}Pb/^{204}Pb$, $^{208}Pb/^{204}Pb$ versus $^{206}Pb/^{204}Pb$. The leachate data considered reliable are plotted as black squares. Small sample size tests at 328 cm and 434 cm are plotted as yellow diamonds. Anthropogenic contamination is suspected for the top section of the core (0-56 cm) and six other samples: the raw data are shown as red triangles and circles, and the data corrected for anthropogenic contamination (assuming a Broken Hill composition) are shown as white triangles and circles. The arrow indicates the approximate direction of mixing towards an anthropogenic contaminant with the composition of Broken Hill (Stacey et al., 1969), from which the data have been corrected onto the mixing line defined by the reliable data.

Table S1: Radiocarbon data for SK129-CR2

Depth (cm)	Sample identification	Species	^{14}C age (yrs)	error	^{14}C age res. corr. (yrs)	Calendar age (yrs BP)	error
2.5	SUERC-13140	*sacculifer*	3727	35	3377	3616	43
12	SUERC-13141	*sacculifer*	6039	35	5689	6462	39
18	SUERC-13142	*sacculifer*	9170	35	8820	9876	107
22	SUERC-13143	*sacculifer*	9038	35	8688	9618	50
26	SUERC-13144	*sacculifer*	11896	38	11546	13411	59
30	SUERC-13147	*sacculifer*	13048	39	12698	14796	88
36	SUERC-13148	*sacculifer*	14341	43	13991	16320	126
40	SUERC-13149	*sacculifer*	14117	42	13767	16026	118
44	SUERC-13150	*sacculifer*	14909	44	14559	17249	171
52	SUERC-13665	*sacculifer*	17841	61	17491	20677	102
58	ANU-5020*	*menardii*	21580	80	21230	25421	129
64	SUERC-13669	*sacculifer*	22409	94	22059	26536	147
78	SUERC-13671	*ruber*	28849	189	28499	33888	248

Notes:
Radiocarbon analysis of planktonic foraminifera at the Scottish Universities Environmental Research Centre (SUERC) AMS Facility (5MV NEC AMS), except for sample at 58 cm (denoted by *) which was picked by Luke Skinner and run by Stewart Fallon at the Australian National University AMS Lab. SUERC analyses were funded by grant allocation 1198.1006. Samples were hydrolysed to CO_2 using 85% orthophosphoric acid at 25℃. The gas was converted to graphite by Fe/Zn reduction. The errors are reported as 1σ. Conversion applied a uniform 350 y reservoir correction (Butzin et al., 2005; Cao et al., 2007) and was converted to calendar years using the Fairbanks et al. (2005) calibration curve 01.07 (see http://radiocarbon.LDEO.columbia.edu). These data were originally presented in Piotrowski et al. (2009), but there was an error in how the reservoir correction was applied which has been corrected here.

Table S2: Benthic oxygen isotope data from SK129-CR2

Depth (cm)	Age (ka BP)	$\delta^{18}O_{Cib}$ Piotrowski et al. 2009	$\delta^{18}O_{Cib}$ Wilson et al. 2015	$\delta^{18}O_{Cib}$ combined
0	2.28	2.88		**2.88**
8	5.26	2.55		**2.55**
14	7.28	2.72		**2.72**
16	8.10	3.31		**3.31**
18	8.93	3.41		**3.41**
22	10.97	3.84		**3.84**
24	12.19	4.01		**4.01**
26	13.41	4.16		**4.16**
30	14.80	4.14		**4.14**
32	15.14	4.04		**4.04**
36	15.83	4.53		**4.53**
40	16.53	4.15		**4.15**
44	17.25	4.16		**4.16**
48	18.96	4.22		**4.22**
52	20.68	4.13		**4.13**
56	23.84	4.20		**4.20**
58	25.42	4.12		**4.12**
60	25.79	3.96		**3.96**
62	26.16	4.10		**4.10**
64	26.54	4.01		**4.01**
66	27.59	4.22		**4.22**
68	28.64	4.24		**4.24**
70	29.69	3.62		**3.62**
72	30.74	3.79		**3.79**
74	31.79	3.77		**3.77**
76	32.84	3.88		**3.88**
78	33.89	3.76		**3.76**
80	34.89	3.78		**3.78**
82	35.89	3.77		**3.77**
84	36.90	3.81		**3.81**
86	37.90	3.93		**3.93**
88	38.90	3.90		**3.90**
90	39.91	3.81		**3.81**
92	40.91	3.93		**3.93**
94	41.91	3.84		**3.84**
96	42.91	3.89		**3.89**
98	43.92	3.53		**3.53**
100	44.92	3.65		**3.65**
102	45.92	3.69		**3.69**
104	46.93	3.67		**3.67**
106	47.93	3.59		**3.59**
108	48.93	3.68		**3.68**
110	49.93	3.76		**3.76**
112	50.94	3.73		**3.73**
114	51.94	3.66		**3.66**
116	52.94	3.80		**3.80**
118	53.95	3.60		**3.60**
120	54.95	3.63		**3.63**

124	56.95	3.59		**3.59**
132	60.97	3.71		**3.71**
140	64.98	3.94		**3.94**
142	65.98	4.09		**4.09**
144	66.98	4.36		**4.36**
146	67.99	3.98		**3.98**
148	68.99	4.18		**4.18**
150	69.99	3.77		**3.77**
152	70.99	3.87		**3.87**
154	72.00	3.85		**3.85**
156	73.00	3.57		**3.57**
160	75.00	3.38		**3.38**
162	76.16	4.07		**4.07**
164	77.33	3.53		**3.53**
166	78.49	3.28		**3.28**
168	79.65	3.21		**3.21**
170	80.82	3.21		**3.21**
172	81.98	3.41		**3.41**
174	83.14	3.32		**3.32**
178	85.47		3.33	**3.33**
186	90.12	3.42		**3.42**
194	94.78	3.12		**3.12**
198	97.10		3.21	**3.21**
210	104.08	3.15		**3.15**
214	106.41	3.31		**3.31**
218	108.73	3.29		**3.29**
222	111.06	3.45		**3.45**
224	112.22	3.33		**3.33**
228	114.55	2.85		**2.85**
232	116.88	3.08		**3.08**
236	119.20	3.18		**3.18**
240	121.53	2.88		**2.88**
242	122.69	2.71		**2.71**
244	123.86	2.88		**2.88**
248	126.18	3.34		**3.34**
250	127.35	2.70		**2.70**
252	128.51	2.86		**2.86**
254	129.67	2.21		**2.21**
256	130.84	3.44		**3.44**
258	132.00	2.44		**2.44**
260	132.83	3.89		**3.89**
262	133.66	4.21		**4.21**
264	134.49	4.01		**4.01**
266	135.32	4.18		**4.18**
270	136.99	4.13		**4.13**
274	138.65	4.40		**4.40**
278	140.31	4.27		**4.27**
282	141.97	4.14		**4.14**
286	143.63	4.30		**4.30**
290	145.30	4.19		**4.19**
294	146.96	4.11		**4.11**
298	148.62	4.15		**4.15**

300	149.45	4.17		**4.17**
306	151.94	4.33		**4.33**
320	157.76		4.13	**4.13**
326	160.25		4.09	**4.09**
334	163.58		3.75	**3.75**
342	166.90		4.11	**4.11**
344	167.73		3.78	**3.78**
344	167.73		3.95	**3.95**
346	168.56		3.80	**3.80**
350	170.23		3.77	**3.77**
352	171.06		3.79	**3.79**
356	172.72		3.78	**3.78**
358	173.55		3.84	**3.84**
364	176.04		3.89	**3.89**
366	176.87		3.89	**3.89**
374	180.20		3.97	**3.97**
378	181.86		3.82	**3.82**
380	182.69		3.63	**3.63**
382	183.52		3.97	**3.97**
384	184.35		3.86	**3.86**
386	185.18		3.91	**3.91**
390	186.85		3.91	**3.91**
392	187.68		3.71	**3.71**
394	188.51		3.84	**3.84**
396	189.34		3.44	**3.44**
400	191.00		3.55	**3.55**
402	192.42		3.21	**3.21**
402	192.42		3.31	**3.31**
404	193.84		3.42	**3.42**
408	196.68		3.28	**3.28**
410	198.11		3.60	**3.60**
412	199.53		3.20	**3.20**
414	200.95		3.18	**3.18**
416	202.37		3.10	**3.10**
418	203.79		3.00	**3.00**
420	205.21		3.06	**3.06**
422	206.63		3.33	**3.33**
424	208.05		3.31	**3.31**
426	209.47		3.17	**3.17**
426	209.47		3.49	**3.49**
428	210.89		3.21	**3.21**
432	213.74		2.97	**2.97**
438	218.00		3.18	**3.18**
444	220.14		3.67	**3.67**
446	220.86		2.93	**2.93**
450	222.29		3.61	**3.61**
456	224.43		3.57	**3.57**
462	226.57		3.48	**3.48**
468	228.71		3.62	**3.62**
474	230.86		3.61	**3.61**
480	233.00		3.40	**3.40**
484	235.40		3.38	**3.38**

488	237.80		3.11	**3.11**
490	239.00		3.20	**3.20**
490	239.00		3.28	**3.28**
494	241.40		2.78	**2.78**
498	243.80		3.06	**3.06**
500	245.00		3.70	**3.70**
504	246.43		3.90	**3.90**
508	247.86		3.88	**3.88**
512	249.29		3.88	**3.88**
518	251.43		3.88	**3.88**

Notes:
All oxygen isotope data are from *C. wuellerstorfi*, either from Piotrowski et al. (2009) or Wilson et al. (2015). Measurements were made in the Godwin Laboratory on *Cibicidoides wuellerstorfi* (> 212 µm). Foraminifera (typically 2 to 5 specimens) were transferred into sample vials, crushed, and soaked in a solution of 3 % hydrogen peroxide for 30 minutes before being removed. After an acetone ultrasonic bath, the samples were dried at 50 °C overnight. The samples were analysed using a Micromass Multicarb Sample Preparation System attached to a VG SIRA or VG PRISM mass spectrometer. Each run of 30 samples was accompanied by 10 reference carbonates and 2 control samples. The results are reported with reference to the international standard Vienna PeeDee Belemnite (VPDB) and the precision is better than ± 0.08 ‰ for $\delta^{18}O$.

Table S3: Age model tie points for SK129-CR2

Depth (cm)	Calendar age (ka BP)	Sed rate below (cm/ka)	Method	Notes
2.5	3.616	3.34	^{14}C	
12	6.462	2.44	^{14}C	
20	9.747	1.64	^{14}C	average of two closely spaced ^{14}C measurements
26	13.411	2.89	^{14}C	
30	14.796	5.81	^{14}C	
38	16.173	5.58	^{14}C	average of two closely spaced ^{14}C measurements
44	17.249	2.33	^{14}C	
52	20.677	1.26	^{14}C	
58	25.421	5.38	^{14}C	
64	26.536	1.90	^{14}C	
78	33.888	1.99	^{14}C	
156	73	2.00	MIS 4/5	
160	75	1.72	YTT	first appearance of Youngest Toba Tuff
258	132	2.41	MIS 5/6	
400	191	1.41	MIS 6/7	
438	218	2.80	MIS 7.3/7.4	
480	233	1.67	MIS 7.4/7.5	
500	245	2.80	MIS 7/8	sedimentation rate below MIS 7-8 boundary is unconstrained and based on sedimentation rate in the subsequent glacial period MIS 7.4

Notes:
The age model is constrained by radiocarbon dates for 0-34 ka, and thereafter graphical correlation of benthic $\delta^{18}O$ to the LR04 benthic $\delta^{18}O$ stack (Lisiecki and Raymo, 2005). The first appearance of the Youngest Toba Tuff (Banakar, 2005; Mark et al., 2014) also provides an independent age estimate that is consistent with the LR04 based age model.

Table S4: All measured leachate Pb isotope data for SK129-CR2 and ODP 758

Core	Depth	Age	Size	Number	Notes	Measured data						Anthropogenic	Corrected data		
	cm	ka BP	g	leaches		206/204	2σ	207/204	2σ	208/204	2σ	contamination?	206/204	207/204	208/204
SK129-CR2	8	5.26	2.6	6		18.9505	0.0024	15.7574	0.0022	39.2759	0.0063	possible	19.1058	15.7764	39.4934
SK129-CR2	12	6.46	2.3	5		18.9950	0.0009	15.7619	0.0011	39.3386	0.0034	possible	19.0983	15.7745	39.4816
SK129-CR2	16	8.10	2.3	6		18.9771	0.0024	15.7564	0.0022	39.3190	0.0063	possible	19.0723	15.7679	39.4410
SK129-CR2	20	9.75	2.2	5		18.8598	0.0009	15.7401	0.0011	39.1495	0.0034	possible	19.0556	15.7636	39.4147
SK129-CR2	24	12.19	2.2	6		18.8740	0.0024	15.7358	0.0022	39.1601	0.0063	possible	19.0093	15.7518	39.3424
SK129-CR2	28	14.10	2.8	5		18.8832	0.0009	15.7305	0.0011	39.1654	0.0034	possible	18.9612	15.7395	39.2671
SK129-CR2	32	15.14	3.3	6		18.7867	0.0024	15.7197	0.0022	39.0406	0.0063	possible	18.9641	15.7403	39.2718
SK129-CR2	36	15.83	3.1	5		18.8672	0.0009	15.7254	0.0011	39.1361	0.0034	possible	18.9371	15.7334	39.2295
SK129-CR2	40	16.53	1.4	6		18.8765	0.0024	15.7203	0.0022	39.1422	0.0063	possible	18.8934	15.7222	39.1612
SK129-CR2	44	17.25	3.1	5		18.8390	0.0009	15.7204	0.0011	39.0869	0.0034	possible	18.9247	15.7302	39.2100
SK129-CR2	52	20.68	1.4	6		18.8632	0.0024	15.7190	0.0022	39.1293	0.0063	possible	18.8944	15.7225	39.1628
SK129-CR2	56	23.84	3.1	5		18.8847	0.0009	15.7252	0.0011	39.1608	0.0034	possible	18.9217	15.7294	39.2054
SK129-CR2	60	25.79	2.8	6		18.9160	0.0024	15.7282	0.0022	39.2021	0.0063				
SK129-CR2	62	26.16	2.8	5		18.9146	0.0009	15.7260	0.0011	39.1937	0.0034				
SK129-CR2	64	26.54	3.3	5		18.9270	0.0009	15.7300	0.0011	39.2159	0.0034				
SK129-CR2	66	27.59	3.2	5		18.9253	0.0009	15.7289	0.0011	39.2065	0.0034				
SK129-CR2	68	28.64	3.6	6		18.9289	0.0024	15.7334	0.0022	39.2234	0.0063				
SK129-CR2	70	29.69	2.9	5		18.9136	0.0009	15.7283	0.0011	39.1958	0.0034				
SK129-CR2	74	31.79	4.0	6		18.9472	0.0024	15.7369	0.0022	39.2473	0.0063				
SK129-CR2	78	33.89	2.6	5		18.9472	0.0009	15.7350	0.0011	39.2425	0.0034				
SK129-CR2	80	34.89	3.0	6		18.9458	0.0024	15.7354	0.0022	39.2445	0.0063				
SK129-CR2	86	37.90	2.9	5		18.9038	0.0009	15.7282	0.0011	39.1793	0.0034				
SK129-CR2	92	40.91	2.0	4		18.9224	0.0018	15.7310	0.0038	39.2135	0.0082				
SK129-CR2	100	44.92	3.0	6		18.9308	0.0024	15.7327	0.0022	39.2181	0.0063				
SK129-CR2	106	47.93	2.6	4		18.9383	0.0018	15.7369	0.0038	39.2440	0.0082				
SK129-CR2	110	49.93	2.7	5		18.8734	0.0009	15.7307	0.0011	39.1423	0.0034	contaminated	18.9713	15.7421	39.2830
SK129-CR2	116	52.94	2.4	6		18.9510	0.0024	15.7375	0.0022	39.2574	0.0063				
SK129-CR2	126	57.96	2.6	4		18.9526	0.0018	15.7380	0.0038	39.2585	0.0082				
SK129-CR2	136	62.97	4.6	5		18.9324	0.0009	15.7349	0.0011	39.2299	0.0034				
SK129-CR2	144	66.98	4.7	5		18.9556	0.0009	15.7362	0.0011	39.2590	0.0034				
SK129-CR2	148	68.99	4.8	6		18.9221	0.0024	15.7379	0.0022	39.2177	0.0063				
SK129-CR2	152	70.99	4.5	5		18.9500	0.0009	15.7441	0.0011	39.2813	0.0034				
SK129-CR2	156	73.00	5.1	6		18.9888	0.0024	15.7494	0.0022	39.3399	0.0063				
SK129-CR2	160	75.00	4.1	5		18.9779	0.0009	15.7471	0.0011	39.3086	0.0034				
SK129-CR2	162	76.16	3.0	6		19.0084	0.0024	15.7547	0.0022	39.3546	0.0063				
SK129-CR2	164	77.33	3.2	5		18.9792	0.0009	15.7524	0.0011	39.3061	0.0034				
SK129-CR2	168	79.65	2.9	6		19.0280	0.0024	15.7588	0.0022	39.3750	0.0063				
SK129-CR2	178	85.47	6.6	5		19.0369	0.0018	15.7594	0.0038	39.3770	0.0082				

SK129-CR2	182	87.80	3.3	5		19.0451	0.0009	15.7590	0.0011	39.3887	0.0034				
SK129-CR2	190	92.45	2.7	6		19.0356	0.0024	15.7600	0.0022	39.3844	0.0063				
SK129-CR2	198	97.10	6.0	5		19.0466	0.0018	15.7621	0.0038	39.4002	0.0082				
SK129-CR2	202	99.43	2.5	5		19.0438	0.0009	15.7640	0.0011	39.3938	0.0034				
SK129-CR2	210	104.08	2.7	6		18.7709	0.0024	15.7365	0.0022	39.0596	0.0063	contaminated	19.1149	15.7787	39.5075
SK129-CR2	212	105.24	1.9	5		19.0736	0.0018	15.7615	0.0038	39.4134	0.0082				
SK129-CR2	216	107.57	1.9	5		19.0747	0.0018	15.7591	0.0038	39.4065	0.0082				
SK129-CR2	224	112.22	2.3	5		19.0498	0.0018	15.7653	0.0038	39.3995	0.0082				
SK129-CR2	230	115.71	3.0	6		19.0408	0.0024	15.7640	0.0022	39.4050	0.0063				
SK129-CR2	240	121.53	3.4	6		19.0291	0.0024	15.7616	0.0022	39.3897	0.0063				
SK129-CR2	246	125.02	2.5	5		19.0144	0.0009	15.7580	0.0011	39.3677	0.0034				
SK129-CR2	252	128.51	2.9	5		18.9961	0.0009	15.7541	0.0011	39.3380	0.0034				
SK129-CR2	254	129.67	3.0	6		18.9870	0.0024	15.7500	0.0022	39.3175	0.0063				
SK129-CR2	256	130.84	2.8	5		18.9739	0.0009	15.7453	0.0011	39.2897	0.0034				
SK129-CR2	258	132.00	2.3	6		18.9677	0.0024	15.7433	0.0022	39.2800	0.0063				
SK129-CR2	260	132.83	2.9	5		18.9426	0.0009	15.7417	0.0011	39.2369	0.0034				
SK129-CR2	264	134.49	3.2	6		18.9212	0.0024	15.7305	0.0022	39.1907	0.0063				
SK129-CR2	270	136.99	3.3	6		18.9252	0.0024	15.7274	0.0022	39.1940	0.0063				
SK129-CR2	280	141.14	2.5	4		18.9086	0.0018	15.7281	0.0038	39.1840	0.0082				
SK129-CR2	290	145.30	2.6	4		18.9137	0.0018	15.7249	0.0038	39.1840	0.0082				
SK129-CR2	296	147.79	2.0	4		18.9135	0.0018	15.7263	0.0038	39.1855	0.0082				
SK129-CR2	304	151.11	2.1	4		18.8981	0.0018	15.7204	0.0038	39.1463	0.0082				
SK129-CR2	310	153.61	2.8	4		18.8996	0.0018	15.7230	0.0038	39.1583	0.0082				
SK129-CR2	320	157.76	3.8	9		18.9053	0.0012	15.7164	0.0013	39.1571	0.0040				
SK129-CR2	328	161.08	4.6	10	L	18.9173	0.0010	15.7253	0.0010	39.1849	0.0021				
SK129-CR2	328	161.08	1.9	10	S	18.8983	0.0010	15.7198	0.0010	39.1632	0.0021				
SK129-CR2	334	163.58	3.4	9		18.9348	0.0012	15.7222	0.0013	39.2066	0.0040				
SK129-CR2	344	167.73	3.0	10		18.9565	0.0010	15.7346	0.0010	39.2537	0.0021				
SK129-CR2	350	170.23	2.7	10		18.9617	0.0010	15.7346	0.0010	39.2576	0.0021				
SK129-CR2	358	173.55	3.2	10		18.9665	0.0033	15.7353	0.0031	39.2634	0.0095				
SK129-CR2	358	173.55	3.2	10	rep	18.9717	0.0034	15.7389	0.0025	39.2769	0.0079				
SK129-CR2	366	176.87	2.7	9		18.9739	0.0012	15.7415	0.0013	39.2794	0.0040				
SK129-CR2	372	179.37	6.7	5	*	18.8642	0.0018	15.7260	0.0038	39.1272	0.0082	contaminated	18.9442	15.7352	39.2406
SK129-CR2	378	181.86	6.0	9		18.9711	0.0012	15.7426	0.0013	39.3065	0.0040				
SK129-CR2	386	185.18	4.8	9		18.9909	0.0012	15.7480	0.0013	39.3355	0.0040				
SK129-CR2	394	188.51	4.9	9		19.0108	0.0012	15.7531	0.0013	39.3641	0.0040				
SK129-CR2	404	193.84	3.4	11		19.0374	0.0033	15.7604	0.0031	39.4120	0.0095				
SK129-CR2	404	193.84	3.4	11	rep	19.0361	0.0034	15.7591	0.0025	39.4090	0.0079				
SK129-CR2	408	196.68	7.0	5	*	19.0723	0.0018	15.7704	0.0038	39.4533	0.0082				
SK129-CR2	414	200.95	3.7	11		19.1210	0.0033	15.7783	0.0031	39.5095	0.0095				
SK129-CR2	414	200.95	3.7	11	rep	19.1214	0.0034	15.7779	0.0025	39.5091	0.0079				
SK129-CR2	418	203.79	2.4	5		19.1083	0.0009	15.7745	0.0011	39.4831	0.0034				

SK129-CR2	422	206.63	7.6	5	*	19.0702	0.0018	15.7688	0.0038	39.4409	0.0082				
SK129-CR2	424	208.05	3.6	9		18.4534	0.0012	15.6961	0.0013	38.6685	0.0040	contaminated	19.1021	15.7755	39.4874
SK129-CR2	426	209.47	3.0	11		19.0458	0.0033	15.7582	0.0031	39.4041	0.0095				
SK129-CR2	426	209.47	3.0	11	rep	19.0465	0.0034	15.7598	0.0025	39.4074	0.0079				
SK129-CR2	434	215.16	3.0	11	L	18.9589	0.0033	15.7505	0.0031	39.2945	0.0095	contaminated	19.0443	15.7607	39.3971
SK129-CR2	434	215.16	3.0	11	L, rep	18.9582	0.0034	15.7493	0.0025	39.2851	0.0079	contaminated			
SK129-CR2	434	215.16	1.7	11	S	19.0081	0.0033	15.7476	0.0031	39.3417	0.0095				
SK129-CR2	434	215.16	1.7	11	S, rep	19.0077	0.0034	15.7469	0.0025	39.3396	0.0079				
SK129-CR2	438	218.00	5.3	5	*	19.0359	0.0018	15.7580	0.0038	39.3829	0.0082				
SK129-CR2	446	220.86	6.5	5	*	19.0344	0.0005	15.7542	0.0016	39.3607	0.0043				
SK129-CR2	450	222.29	4.7	9		19.0279	0.0012	15.7487	0.0013	39.3388	0.0040				
SK129-CR2	462	226.57	5.5	5	*	19.0135	0.0005	15.7516	0.0016	39.3330	0.0043				
SK129-CR2	468	228.71	4.2	9		19.0200	0.0012	15.7517	0.0013	39.3553	0.0040				
SK129-CR2	474	230.86	2.5	11		18.9960	0.0033	15.7484	0.0031	39.3327	0.0095				
SK129-CR2	474	230.86	2.5	11	rep	19.0002	0.0034	15.7505	0.0025	39.3407	0.0079				
SK129-CR2	484	235.40	7.9	5	*	19.0219	0.0005	15.7570	0.0016	39.3683	0.0043				
SK129-CR2	488	237.80	2.7	11		19.0307	0.0033	15.7582	0.0031	39.3822	0.0095				
SK129-CR2	488	237.80	2.7	11	rep	19.0295	0.0034	15.7573	0.0025	39.3768	0.0079				
SK129-CR2	494	241.40	3.0	5	*	19.0212	0.0005	15.7573	0.0016	39.3633	0.0043				
SK129-CR2	498	243.80	2.7	11		18.9920	0.0033	15.7464	0.0031	39.3165	0.0095				
SK129-CR2	498	243.80	2.7	11	rep	18.9924	0.0034	15.7461	0.0025	39.3157	0.0079				
SK129-CR2	504	246.43	3.2	11		18.9714	0.0033	15.7424	0.0031	39.2912	0.0095				
SK129-CR2	504	246.43	3.2	11	rep	18.9676	0.0034	15.7365	0.0025	39.2719	0.0079				
SK129-CR2	508	247.86	1.8	9		18.9606	0.0012	15.7284	0.0013	39.2484	0.0040				
SK129-CR2	512	249.29	3.9	11		18.7316	0.0033	15.7150	0.0031	38.9328	0.0095	contaminated	18.9775	15.7437	39.2926
SK129-CR2	512	249.29	3.9	11	rep	18.7307	0.0034	15.7136	0.0025	38.9286	0.0079	contaminated			
SK129-CR2	518	251.43	5.6	5	*	18.9247	0.0005	15.7266	0.0016	39.2017	0.0043				
ODP 758 A1 H1 67-69	67	33	13.2	6		19.0040	0.0011	15.7391	0.0016	39.2354	0.0049				
ODP 758 A1 H2 64.5-67	214.5	77	7.3	6		18.9620	0.0011	15.7481	0.0016	39.3243	0.0049				
ODP 758 A1 H2 123.5-125.5	273.5	128	9.1	6		18.9767	0.0011	15.7558	0.0016	39.3633	0.0049				
ODP 758 A1 H3 13-15.5	313	143	9.3	6		18.8993	0.0005	15.7258	0.0016	39.2116	0.0043				
ODP 758 A1 H3 94-96	394	192	9.4	6		18.9877	0.0018	15.7515	0.0038	39.3609	0.0082				
ODP 758 A1 H4 8-10	458	233	8.6	6		18.9868	0.0018	15.7544	0.0038	39.3608	0.0082				
ODP 758 A1 H4 37-39	487	249	9.2	6		18.9376	0.0018	15.7389	0.0038	39.2859	0.0082				

Notes:

This table contains all measured data and data after correction for anthropogenic contamination where contamination was suspected.

Core	Identifiers for ODP Leg 121 Site 758 are Hole, Core, Type, Section, Interval
Depth	Depth in cm below sea floor
Size (g)	Wet weights after decarbonation
Number leaches	Number of times leached in ~30 mL acetic acid before HH leaching

L	Large sample size test
S	Small sample size test
rep	Mass spectrometry replicate
*	Leached using low solution/solid ratios to prevent complete decarbonation before HH leaching
possible	Samples where a small anthropogenic contamination is suspected; followed by data corrected as described in Supplementary Information
contaminated	Samples with clear anthropogenic contamination identified; followed by data corrected as described in Supplementary Information
2σ	Uncertainties are based on the standard deviation (2σ) of repeat measurements of concentration-matched NIST-SRM-981 in each analytical session. Long term reproducibility (2σ) assessed from two internal standards (leachate samples) is 140 ppm for $^{206}Pb/^{204}Pb$, 160 ppm for $^{207}Pb/^{204}Pb$ and 190 ppm for $^{208}Pb/^{204}Pb$

Table S5: Leachate Pb isotope data for plotting for SK129-CR2

Core	Depth cm	Age ka BP	Size g	Notes	206/204	2σ	207/204	2σ	208/204	2σ
SK129-CR2	8	5.26	2.6	corrected	19.1058	0.0024	15.7764	0.0022	39.4934	0.0063
SK129-CR2	12	6.46	2.3	corrected	19.0983	0.0009	15.7745	0.0011	39.4816	0.0034
SK129-CR2	16	8.10	2.3	corrected	19.0723	0.0024	15.7679	0.0022	39.4410	0.0063
SK129-CR2	20	9.75	2.2	corrected	19.0556	0.0009	15.7636	0.0011	39.4147	0.0034
SK129-CR2	24	12.19	2.2	corrected	19.0093	0.0024	15.7518	0.0022	39.3424	0.0063
SK129-CR2	28	14.10	2.8	corrected	18.9612	0.0009	15.7395	0.0011	39.2671	0.0034
SK129-CR2	32	15.14	3.3	corrected	18.9641	0.0024	15.7403	0.0022	39.2718	0.0063
SK129-CR2	36	15.83	3.1	corrected	18.9371	0.0009	15.7334	0.0011	39.2295	0.0034
SK129-CR2	40	16.53	1.4	corrected	18.8934	0.0024	15.7222	0.0022	39.1612	0.0063
SK129-CR2	44	17.25	3.1	corrected	18.9247	0.0009	15.7302	0.0011	39.2100	0.0034
SK129-CR2	52	20.68	1.4	corrected	18.8944	0.0024	15.7225	0.0022	39.1628	0.0063
SK129-CR2	56	23.84	3.1	corrected	18.9217	0.0009	15.7294	0.0011	39.2054	0.0034
SK129-CR2	60	25.79	2.8		18.9160	0.0024	15.7282	0.0022	39.2021	0.0063
SK129-CR2	62	26.16	2.8		18.9146	0.0009	15.7260	0.0011	39.1937	0.0034
SK129-CR2	64	26.54	3.3		18.9270	0.0009	15.7300	0.0011	39.2159	0.0034
SK129-CR2	66	27.59	3.2		18.9253	0.0009	15.7289	0.0011	39.2065	0.0034
SK129-CR2	68	28.64	3.6		18.9289	0.0024	15.7334	0.0022	39.2234	0.0063
SK129-CR2	70	29.69	2.9		18.9136	0.0009	15.7283	0.0011	39.1958	0.0034
SK129-CR2	74	31.79	4.0		18.9472	0.0024	15.7369	0.0022	39.2473	0.0063
SK129-CR2	78	33.89	2.6		18.9472	0.0009	15.7350	0.0011	39.2425	0.0034
SK129-CR2	80	34.89	3.0		18.9458	0.0024	15.7354	0.0022	39.2445	0.0063
SK129-CR2	86	37.90	2.9		18.9038	0.0009	15.7282	0.0011	39.1793	0.0034
SK129-CR2	92	40.91	2.0		18.9224	0.0018	15.7310	0.0038	39.2135	0.0082
SK129-CR2	100	44.92	3.0		18.9308	0.0024	15.7327	0.0022	39.2181	0.0063
SK129-CR2	106	47.93	2.6		18.9383	0.0018	15.7369	0.0038	39.2440	0.0082
SK129-CR2	116	52.94	2.4		18.9510	0.0024	15.7375	0.0022	39.2574	0.0063
SK129-CR2	126	57.96	2.6		18.9526	0.0018	15.7380	0.0038	39.2585	0.0082
SK129-CR2	136	62.97	4.6		18.9324	0.0009	15.7349	0.0011	39.2299	0.0034
SK129-CR2	144	66.98	4.7		18.9556	0.0009	15.7362	0.0011	39.2590	0.0034
SK129-CR2	148	68.99	4.8		18.9221	0.0024	15.7379	0.0022	39.2177	0.0063
SK129-CR2	152	70.99	4.5		18.9500	0.0009	15.7441	0.0011	39.2813	0.0034
SK129-CR2	156	73.00	5.1		18.9888	0.0024	15.7494	0.0022	39.3399	0.0063
SK129-CR2	160	75.00	4.1		18.9779	0.0009	15.7471	0.0011	39.3086	0.0034
SK129-CR2	162	76.16	3.0		19.0084	0.0024	15.7547	0.0022	39.3546	0.0063
SK129-CR2	164	77.33	3.2		18.9792	0.0009	15.7524	0.0011	39.3061	0.0034
SK129-CR2	168	79.65	2.9		19.0280	0.0024	15.7588	0.0022	39.3750	0.0063
SK129-CR2	178	85.47	6.6		19.0369	0.0018	15.7594	0.0038	39.3770	0.0082
SK129-CR2	182	87.80	3.3		19.0451	0.0009	15.7590	0.0011	39.3887	0.0034
SK129-CR2	190	92.45	2.7		19.0356	0.0024	15.7600	0.0022	39.3844	0.0063
SK129-CR2	198	97.10	6.0		19.0466	0.0018	15.7621	0.0038	39.4002	0.0082
SK129-CR2	202	99.43	2.5		19.0438	0.0009	15.7640	0.0011	39.3938	0.0034
SK129-CR2	212	105.24	1.9		19.0736	0.0018	15.7615	0.0038	39.4134	0.0082
SK129-CR2	216	107.57	1.9		19.0747	0.0018	15.7591	0.0038	39.4065	0.0082
SK129-CR2	224	112.22	2.3		19.0498	0.0018	15.7653	0.0038	39.3995	0.0082
SK129-CR2	230	115.71	3.0		19.0408	0.0024	15.7640	0.0022	39.4050	0.0063
SK129-CR2	240	121.53	3.4		19.0291	0.0024	15.7616	0.0022	39.3897	0.0063
SK129-CR2	246	125.02	2.5		19.0144	0.0009	15.7580	0.0011	39.3677	0.0034

SK129-CR2	252	128.51	2.9	18.9961	0.0009	15.7541	0.0011	39.3380	0.0034
SK129-CR2	254	129.67	3.0	18.9870	0.0024	15.7500	0.0022	39.3175	0.0063
SK129-CR2	256	130.84	2.8	18.9739	0.0009	15.7453	0.0011	39.2897	0.0034
SK129-CR2	258	132.00	2.3	18.9677	0.0024	15.7433	0.0022	39.2800	0.0063
SK129-CR2	260	132.83	2.9	18.9426	0.0009	15.7417	0.0011	39.2369	0.0034
SK129-CR2	264	134.49	3.2	18.9212	0.0024	15.7305	0.0022	39.1907	0.0063
SK129-CR2	270	136.99	3.3	18.9252	0.0024	15.7274	0.0022	39.1940	0.0063
SK129-CR2	280	141.14	2.5	18.9086	0.0018	15.7281	0.0038	39.1840	0.0082
SK129-CR2	290	145.30	2.6	18.9137	0.0018	15.7249	0.0038	39.1840	0.0082
SK129-CR2	296	147.79	2.0	18.9135	0.0018	15.7263	0.0038	39.1855	0.0082
SK129-CR2	304	151.11	2.1	18.8981	0.0018	15.7204	0.0038	39.1463	0.0082
SK129-CR2	310	153.61	2.8	18.8996	0.0018	15.7230	0.0038	39.1583	0.0082
SK129-CR2	320	157.76	3.8	18.9053	0.0012	15.7164	0.0013	39.1571	0.0040
SK129-CR2	328	161.08	4.6	18.9173	0.0010	15.7253	0.0010	39.1849	0.0021
SK129-CR2	334	163.58	3.4	18.9348	0.0012	15.7222	0.0013	39.2066	0.0040
SK129-CR2	344	167.73	3.0	18.9565	0.0010	15.7346	0.0010	39.2537	0.0021
SK129-CR2	350	170.23	2.7	18.9617	0.0010	15.7346	0.0010	39.2576	0.0021
SK129-CR2	358	173.55	3.2	18.9665	0.0033	15.7353	0.0031	39.2634	0.0095
SK129-CR2	366	176.87	2.7	18.9739	0.0012	15.7415	0.0013	39.2794	0.0040
SK129-CR2	378	181.86	6.0	18.9711	0.0012	15.7426	0.0013	39.3065	0.0040
SK129-CR2	386	185.18	4.8	18.9909	0.0012	15.7480	0.0013	39.3355	0.0040
SK129-CR2	394	188.51	4.9	19.0108	0.0012	15.7531	0.0013	39.3641	0.0040
SK129-CR2	404	193.84	3.4	19.0374	0.0033	15.7604	0.0031	39.4120	0.0095
SK129-CR2	408	196.68	7.0	19.0723	0.0018	15.7704	0.0038	39.4533	0.0082
SK129-CR2	414	200.95	3.7	19.1210	0.0033	15.7783	0.0031	39.5095	0.0095
SK129-CR2	418	203.79	2.4	19.1083	0.0009	15.7745	0.0011	39.4831	0.0034
SK129-CR2	422	206.63	7.6	19.0702	0.0018	15.7688	0.0038	39.4409	0.0082
SK129-CR2	426	209.47	3.0	19.0458	0.0033	15.7582	0.0031	39.4041	0.0095
SK129-CR2	438	218.00	5.3	19.0359	0.0018	15.7580	0.0038	39.3829	0.0082
SK129-CR2	446	220.86	6.5	19.0344	0.0005	15.7542	0.0016	39.3607	0.0043
SK129-CR2	450	222.29	4.7	19.0279	0.0012	15.7487	0.0013	39.3388	0.0040
SK129-CR2	462	226.57	5.5	19.0135	0.0005	15.7516	0.0016	39.3330	0.0043
SK129-CR2	468	228.71	4.2	19.0200	0.0012	15.7517	0.0013	39.3553	0.0040
SK129-CR2	474	230.86	2.5	18.9960	0.0033	15.7484	0.0031	39.3327	0.0095
SK129-CR2	484	235.40	7.9	19.0219	0.0005	15.7570	0.0016	39.3683	0.0043
SK129-CR2	488	237.80	2.7	19.0307	0.0033	15.7582	0.0031	39.3822	0.0095
SK129-CR2	494	241.40	3.0	19.0212	0.0005	15.7573	0.0016	39.3633	0.0043
SK129-CR2	498	243.80	2.7	18.9920	0.0033	15.7464	0.0031	39.3165	0.0095
SK129-CR2	504	246.43	3.2	18.9714	0.0033	15.7424	0.0031	39.2912	0.0095
SK129-CR2	508	247.86	1.8	18.9606	0.0012	15.7284	0.0013	39.2484	0.0040
SK129-CR2	518	251.43	5.6	18.9247	0.0005	15.7266	0.0016	39.2017	0.0043

Notes:

This table contains the data considered reliable and most appropriate for plotting.

Replicate data (rep in Table S4) and data from small samples (S in Table S4) have been removed.

Where anthropogenic contamination was identified (contaminated in Table S4) the data have also been removed.

For 8-56 cm the data included here are the data corrected for minor anthropogenic contamination.

Uncertainties are based on the standard deviation (2σ) of repeat measurements of concentration matched NIST-SRM-981 in each analytical session. Long term reproducibility (2σ) assessed from two internal leachate samples is 140 ppm for $^{206}Pb/^{204}Pb$, 160 ppm for $^{207}Pb/^{204}Pb$ and 190 ppm for $^{208}Pb/^{204}Pb$

Supplementary references

Abouchami, W., Galer, S.J.G., Hofmann, A.W., 2000. High precision lead isotope systematics of lavas from the Hawaiian Scientific Drilling Project. Chemical Geology 169, 187-209.

Banakar, V.K., 2005. $\delta^{13}C$ depleted oceans before the Termination 2: More nutrient-rich deep-water formation or light-carbon transfer? Indian J. Mar. Sci. 34, 249-258.

Belshaw, N.S., Freedman, P.A., O'Nions, R.K., Frank, M., Guo, Y., 1998. A new variable dispersion double-focusing plasma mass spectrometer with performance illustrated for Pb isotopes. Int. J. Mass Spectrom. 181, 51-58.

Butzin, M., Prange, M., Lohmann, G., 2005. Radiocarbon simulations for the glacial ocean: The effects of wind stress, Southern Ocean sea ice and Heinrich events. Earth Planet. Sci. Lett. 235, 45-61.

Cao, L., Fairbanks, R.G., Mortlock, R.A., Risk, M.J., 2007. Radiocarbon reservoir age of high latitude North Atlantic surface water during the last deglacial. Quat. Sci. Rev. 26, 732-742.

Fairbanks, R.G., Mortlock, R.A., Chiu, T.C., Cao, L., Kaplan, A., Guilderson, T.P., Fairbanks, T.W., Bloom, A.L., Grootes, P.M., Nadeau, M.J., 2005. Radiocarbon calibration curve spanning 0 to 50,000 years BP based on paired $^{230}Th/^{234}U/^{238}U$ and ^{14}C dates on pristine corals. Quat. Sci. Rev. 24, 1781-1796.

Galer, S.J.G., Abouchami, W., 1998. Practical application of lead triple spiking for correction of instrumental mass discrimination. Mineralogical Magazine 62A, 491-492.

Galy, A., France-Lanord, C., 2001. Higher erosion rates in the Himalaya: Geochemical constraints on riverine fluxes. Geology 29, 23-26.

Gutjahr, M., Frank, M., Stirling, C.H., Klemm, V., van de Flierdt, T., Halliday, A.N., 2007. Reliable extraction of a deepwater trace metal isotope signal from Fe-Mn oxyhydroxide coatings of marine sediments. Chemical Geology 242, 351-370.

Hirata, T., 1996. Lead isotopic analyses of NIST standard reference materials using multiple collector inductively coupled plasma mass spectrometry coupled with a modified external correction method for mass discrimination effect. Analyst 121, 1407-1411.

Kamenov, G.D., Mueller, P.A., Perfit, M.R., 2004. Optimization of mixed Pb-Tl solutions for high precision isotopic analyses by MC-ICP-MS. J. Anal. At. Spectrom. 19, 1262-1267.

Lisiecki, L.E., Raymo, M.E., 2005. A Pliocene-Pleistocene stack of 57 globally distributed benthic $\delta^{18}O$ records. Paleoceanography 20, doi: 10.1029/2004pa001071.

Mark, D.F., Petraglia, M., Smith, V.C., Morgan, L.E., Barfod, D.N., Ellis, B.S., Pearce, N.J., Pal, J.N., Korisettar, R., 2014. A high-precision $^{40}Ar/^{39}Ar$ age for the Young Toba Tuff and dating of ultra-distal tephra: forcing of Quaternary climate and implications for hominin occupation of India. Quaternary Geochronology 21, 90-103.

Piotrowski, A.M., Banakar, V.K., Scrivner, A.E., Elderfield, H., Galy, A., Dennis, A., 2009. Indian Ocean circulation and productivity during the last glacial cycle. Earth Planet. Sci. Lett. 285, 179-189.

Rehkamper, M., Mezger, K., 2000. Investigation of matrix effects for Pb isotope ratio measurements by multiple collector ICP-MS: verification and application of optimized analytical protocols. J. Anal. At. Spectrom. 15, 1451-1460.

Stacey, J.S., Delevaux, M.E., Ulrych, T.J., 1969. Some triple-filament lead isotope ratio measurements and an absolute growth curve for single-stage leads. Earth Planet. Sci. Lett. 6, 15-25.

van de Velde, K., Vallelonga, P., Candelone, J.P., Rosman, K.J.R., Gaspari, V., Cozzi, G., Barbante, C., Udisti, R., Cescon, P., Boutron, C.F., 2005. Pb isotope record over one century in snow from Victoria Land, Antarctica. Earth Planet. Sci. Lett. 232, 95-108.

Wilson, D.J., Piotrowski, A.M., Galy, A., Banakar, V.K., 2015. Interhemispheric controls on deep ocean circulation and carbon chemistry during the last two glacial cycles. Paleoceanography, doi: 10.1002/2014pa002707

Wilson, D.J., Piotrowski, A.M., Galy, A., Clegg, J.A., 2013. Reactivity of neodymium carriers in deep sea sediments: Implications for boundary exchange and paleoceanography. Geochim. Cosmochim. Acta 109, 197-221.